Comment on:
"Energetics and Kinetics of Thermal Ionization Models of MALDI" by Richard Knochenmuss. *J. Am. Soc. Mass Spectrom*. 25, 1521–1527 (2014)

Thermal proton transfer model was proposed to quantitatively describe the generation of primary ions in matrix-assisted laser desorption ionization [*J. Am. Soc. Mass Spectrom.* 25, 310–318 (2014), ibid 25, 1087-1087 (2014)]. Knochenmuss criticized the calculation methods and assumption used in the thermal proton transfer model [*J. Am. Soc. Mass Spectrom.* **25**, 1521–1527 (2014)]. In this work, we show that Knochenmuss applied the model under conditions not relevant to our conclusions; therefore, we do not accept his argument. We point out also some issues with Knochenmuss' approach to the calculation of dielectric response. We applied the model under suitable conditions, where errors are controlled. Taking into account the application of the model to relevant conditions, and the correct treatment of dielectric response, we find that none of Knochenmuss' criticisms are relevant to MALDI events. We do conclude that the best test of the thermal proton transfer model hypotheses will be obtained from the best available calculation of solvation free energies in a high temperature polar liquid.

Since its inception, matrix-assisted laser desorption ionization has been widely used in mass spectrometry for large nonvolatile and labile molecules. However, the ionization mechanism remains unclear. Recently we adopted the concept of the polar fluid model [1, 2] and developed a thermal proton transfer model to quantitatively describe the generation of primary ions [3–5]. In the thermal proton transfer model, matrix molecules absorb photon energy and convert the majority into thermal energy. The high temperature in the irradiation volume melts the solid into liquid, and also induces chemical reactions. One reaction that can be easily induced through a high temperature is the proton disproportionation reaction, $M + M \rightleftarrows (M - H)^- + (M + H)^+$ (for pure matrix) or $M + A \rightleftarrows (M - H)^- + (A + H)^+$ (for mixture of matrix and analyte) where M and A represent matrix and analyte molecules. We assume that proton disproportionation reactions reach an equilibrium in liquid because of the high collision frequency and low reaction barrier. The ion-to-neutral ratio can be calculated from the equilibrium constant, or the Gibbs free energy and the temperature.

$$\frac{cation}{neutral} = \frac{anion}{neutral} = \sqrt{K} = e^{-\frac{\Delta G_1}{2RT}}$$

The Gibbs free energy of proton disproportionation is low because of the solvation energy. The solvation energy was calculated using a polarizable continuum model, in which the dielectric constant was estimated using the Clausius-Mossotti equation and the Kirkwood-Fröhlich equation. The values of the dipole moment and the static polarizability used in these equations were calculated using an ab initio method. The Kirkwood-Fröhlich equation was replaced by the equation reported by Caillol et al. [6, 7] in our recent study [8, 9], but the results were similar. The ion loss caused by ion–ion recombination after desorption was determined to be low; therefore, the ion-to-neutral ratio in liquid is similar to that after desorption.

Knochenmuss criticized our calculation methods and assumption used in the thermal proton transfer model [10]. These criticisms included (1) the calculation method of the dielectric constant, (2) the assumption of equilibrium for proton disproportionation reaction, and (3) the ion–ion recombination rate in the gas plume. These criticisms are discussed in the following paragraphs.

(1) The calculation method of the dielectric constant

Knochenmuss calculated polarizability as a function of the wavelength (or the reciprocal of frequency) of the applied field. He demonstrated that polarizability is low in long wavelengths (low frequency), and increases rapidly at short wavelengths (high or optical frequency). He then applied the calculated polarizability to the Clausius-Mossotti equation. He showed that the results from the Clausius-Mossotti equation diverge when polarizability is large (near 4.3×10^{-23} cm^3). The divergence in the Clausius-Mossotti equation also resulted in the divergence in the calculation of dielectric constant. He concluded that this method is unsuitable for calculating the dielectric constant. On page 3 of his paper, Column 1, Knochenmuss stated, "As is evident, ab initio calculations of molecular polarizability at optical frequencies are unsuitable for accurate estimation of static dielectric constants of MALDI matrix fluids. Not only is the method physically incomplete but also arbitrary, and very large dielectric constants can be obtained by choice of frequency at which to calculate the polarizability." In making these calculations, Knochenmuss has used the equations incorrectly, outside their range of applicability. He has then concluded that the divergence so obtained shows that the equations should not be used under other conditions. This argument does not hold.

Despite manageable experimental or theoretical obstacles, our theory's predictions contain no ambiguity or inconsistency, and the results are not unreasonably large, nor is there a problematic divergence, when the method is applied correctly. Knochenmuss used the methods under inapplicable conditions, whereas we used these methods under suitable conditions. The "high-frequency" dielectric constant in the Clausius-Mossotti equation is the electrons' contribution to the static dielectric constant. Calling this quantity the "optical" or "high-frequency"

Correspondence to: Chi-Kung Ni; *e-mail:* ckni@po.iams.sinica.edu.tw
© 2015 American Society for Mass Spectrometry
doi:10.1007/s13361-015-1197-8
(J Am Soc Mass Spectrom 2015)

dielectric constant, as Knochenmuss has done, can be misleading. In the rigorous treatment [6], electrons are assumed first to respond instantaneously to an applied field (Equation 4 in [6]), and only later is the high frequency limit taken to obtain the Clausius-Mossotti equation from the static polarizability (Equation 56 and subsequent equations in [6]). This sequence of approximations makes it clear that the polarizability used in the Clausius-Mossotti equation is the static response of the electrons with the nuclei held fixed, a quantity that can be determined from ab initio calculations. It is true that in general there is a connection between the ground state response of a system of electrons and the spectrum of excited states, but this is not relevant here. Ideally, only static polarizability should be utilized in the Clausius-Mossotti equation for use as a step in calculating the total static dielectric; polarizabilities at nonzero frequencies should not be used [6, 7, 11]. The confusion arises here because experimentally the static polarizability is difficult to determine. A common practice is to replace the static polarizability with one obtained from the refractive index at a frequency chosen carefully so that it captures electronic response, but so high that nuclei cannot respond [11]. It follows that the divergence of the polarizability reported by Knochenmuss does not occur in our calculations, as our polarizabilities are obtained from ab initio calculations and are in the relevant sense static responses. Although most textbooks do not explain the reason only static polarizability should be used, using static polarizability in the Clausius-Mossotti equation is a standard practice in physical chemistry textbooks [12, 13]. A more straightforward treatment has been given by Pollock et al. [14], and the connection between macroscopic and molecular dielectric properties is analysed by Madden and Kivelson [15].

In another example, Knochenmuss demonstrated a divergence at $\alpha\rho = 3/(4\pi)$ in the "high-frequency" dielectric constant obtained from the Clausius-Mossotti equation,

$$\frac{\varepsilon_\infty - 1}{\varepsilon_\infty + 2} = \frac{4\pi}{3}\,\alpha\,\rho_N \qquad (1)$$

and the consequent divergence in the total static dielectric constant. In fact, this divergence occurred outside the range of the applicability of the Clausius-Mossotti equation. On the right side of Clausius-Mossotti equation (Equation 1), the terms in $\alpha\rho_N$ of the third and higher orders have been neglected [6]. If $\alpha\rho_N$ is not low [e.g., near $\alpha\rho_N = 3/(4\pi)$], high-order terms should be included, or a more advanced method should be used [6, 7]. This issue is long- and well-known, and a relevant derivation of the Clausius-Mossotti equation was given by Pollock et al [14]. The divergence in the dielectric constant demonstrated by Knochenmuss in his Figure 2 is a mathematical artifact, appearing only when the polarizability was too high for use in the Clausius-Mossotti equation. On the other hand, our theory applied the Clausius-Mossotti equation to a range of sufficiently small static polarizabilities, and that range was sufficient for the molecules of interest.

On page 4 of his article, Column 1, Knochenmuss used values of the dielectric constant of water at a high temperature to try to place limits on the dielectric constant under MALDI conditions. This is misleading because Knochenmuss used data for water in the gas phase. Thermal proton transfer model assumes that ions are stabilized in a dense phase, and that this dense liquid-like state has a high dielectric constant. Using a dielectric constant of gas phase cannot provide sufficient evidence for or against the presence of the liquid-like state. More details on "high-frequency" dielectric constants, the Clausius-Mossotti equation, and the calculation of dielectric constants will be provided in a separate paper [16].

Knochenmuss claimed that the predicted peak MALDI temperature and pressure exceed the critical point of numerous substances, and that the matrix fluid must become supercritical fluids in a MALDI event. He suggested that the dielectric constant of the matrix fluid must be close to that of the supercritical fluids. In fact, phase equilibrium does not exist during the MALD I desorption process, and supercritical fluid does not exist in a MALDI event [3–5]. The so called "liquid phase" in thermal proton transfer model is not the liquid phase in a phase equilibrium. In thermal proton transfer model, the "liquid phase" simply indicates that the structure of the matrix material existed briefly during the change from the initial solid state to the final gas phase. If the molecules have sufficient energy in the rotational and vibrational degrees of freedom after laser irradiation and before desorption, molecules continue to collide with other molecules and are partially free to rotate and vibrate as well as undergo chemical reactions. The structure of such material satisfies the definition of "the liquid phase" in thermal proton transfer model.

The dielectric constant of the matrix is used in thermal proton transfer model to calculate the solvation energy of ions and neutrals. Although the calculation of the dielectric constant may not be very accurate, this inaccuracy does not affect that of thermal proton transfer model substantially because the solvation energy is not sensitive to the dielectric constant when it is high. The solvation energy typically increases rapidly when the dielectric constant rises from 1 to 3, and stabilizes when the dielectric constant is higher than 5. For example, the solvation energies of protonated 2,5-dihydroxybenzoic acid calculated from the polarizable continuum model are 0 kJ/mol, 130 kJ/mol, 158 kJ/mol, and 188 kJ/mol in materials with dielectric constants of 1, 3, 5, and 10, respectively. The calculations in our previous study indicated that the calculated dielectric constants of matrices at high temperatures were sufficiently large to prevent the solvation energy from changing substantially because of the potential inaccuracy of the dielectric constant calculations.

(2) Equilibrium before desorption

In thermal proton transfer model, we assume that proton disproportionation reactions reach equilibrium before desorption [3–5]. Knochenmuss cited [17] and [18] as evidence to demonstrate that these reactions does not reach equilibrium.

The authors in [17] examined the ratios of positive and negative ion yields of MALDI for fibrinopeptide A, angiotensin 1, and bradykinin, in combination with six matrices (CHCA, 2,5-DHB, 4-NA, ATT, ANP, 5-AQ). They then compared the experimental results with the theoretical predictions

based on the equilibrium model for the charge transfer between matrix and analyte ions in the laser ablation plume.

$$(M + H)^+ + A \rightleftarrows (A + H)^+ + M \quad (2)$$

$$(M - H)^- + A \rightleftarrows (A - H)^- + M \quad (3)$$

If Reactions 2 and 3 reach equilibrium, the following equation is obtained:

$$\frac{\lfloor A + H^+ \rfloor}{\lfloor A - H^- \rfloor} = \frac{\lfloor M + H^+ \rfloor}{\lfloor M - H^- \rfloor} \exp\left\{ - \frac{\lfloor GB(M) - GB(M - H^-) \rfloor}{RT} \right\}$$

$$\exp\left\{ - \frac{\lfloor GB(A) - GB(A - H^-) \rfloor}{RT} \right\}$$

For a particular analyte, the relative concentration of protonated and deprotonated analytes can be expressed as

$$\frac{\lfloor A + H^+ \rfloor}{\lfloor A - H^- \rfloor} \propto \exp\left\{ - \frac{\lfloor GB(M) - GB(M - H^-) \rfloor}{RT} \right\} \quad (4)$$

On page 126, Column 1, the authors of [17] listed three assumptions used to obtain Equation 4: (1) the equilibrium of Reactions 2 and 3 has been established; (2) a temperature has been defined; and (3) the proportional factor contains the relative concentration of protonated and deprotonated matrix ions, which are constant. Based on Equation 4, a plot of the logarithm of the ratio of positive to negative analyte ions versus the sum of the gas-phase basicities of the matrices, GB(M) + GB(M − H^-) should yield a straight line with a negative slope (–1/RT). However, no negative slope matching the theoretical predictions was observed in the experimental data. Knochenmuss concluded that Reactions 2 and 3 did not reach equilibrium.

Although the authors in [17] did not examine the equilibrium condition of M + M ⇄ $(M + H)^+$ + $(M - H)^-$ or M + A ⇄ $(A + H)^+$ + $(M - H)^-$ used in thermal proton transfer model, if these reactions reach equilibrium, then Reactions 2 and 3 are also likely to do so. However, the discrepancy between the experimental data and the theoretical predictions in [17] and [18] does not necessarily indicate the nonequilibrium of Reactions 2 and 3 because Equation 4 is based on three assumptions. One assumption that was not satisfied under the experimental conditions is the second. In [17], the authors maintained a constant laser fluence for all of the matrices (page 123, bottom of Column 1). However, a similar laser fluence does not indicate a similar temperature. As demonstrated in Equations 8–11 in [3], the temperature of a matrix after laser irradiation depends on the absorption cross section at the laser wavelength, fluorescence quantum yield, density, and heat capacity. Specifically, the absorption cross-section plays a crucial role in determining the temperature. These parameters of the six matrices used in [17] are not likely to be similar, and the temperatures for these matrices vary. Consequently, the absence of a straight line with a negative slope (–1/RT) in the plot was not completely unexpected, and the discrepancy in experimental data and theoretical predictions does not indicate the nonequilibrium of Reactions 2 and 3.

(3) Ion-ion recombination in the expanding gas plume

Knochenmuss used "black sphere" model to calculate the ion–ion recombination rate [10]. He demonstrated that the fraction of ions that did not undergo ion–ion recombination in the gas plume was only 6×10^{-6}. In fact, "black sphere" model was developed to calculate the kinetics of Frenkel defect recombination and accumulation in ionic solids [19]. This model is not suitable for the calculation of ion–ion recombination in the gas plume.

In our previous research, the ion–ion recombination rate in the gas plume was calculated using the gas kinetic hard sphere collision theory. The fraction of ions lost during ion–ion recombination in the gas plume was determined to be small, and the ion-to-neutral ratio measured in the gas phase was similar to the ion-to-neutral ratio generated in the condensed phase. In the following paragraphs, accurate calculations of ion–ion recombination rate constant using the Langevin-Harper formula and the Thomson formula are presented [20–22]. The results were similar to the results of the hard sphere collision theory.

The neutralization of positive and negative ions is an exothermic reaction. A neutral molecule must collide with a colliding ion pair and remove part of the energy from the ion pair, rendering the energy of the ion pair insufficient for separation again. Three-body collision is crucial in ion–ion recombination in low-pressure regions. As the pressure increases, the frequency of three-body collisions becomes high enough to stabilize every neutralized product. The diffusion of ions toward the ions of opposite signs determines the rate in high-pressure regions. The Langevin-Harper formula and the Thomson formula were derived to calculate the ion–ion recombination rate constants in high-pressure and low-pressure regions, respectively [20–22]. These formulas are accurate within one order of magnitude. Typical ion–ion recombination rate constant increases as pressure increases in low-pressure regions. Recombination rate constant is approximately proportional to pressure, and reaches the maximal value $\sigma_{recom} = 10^{-6}$ cm^3 s^{-1} at a pressure of 100–1000 Torr. The actual values of the maximal rate constant and pressure depend on the size of molecules, molecular weight, and temperature. Above 1000 Torr, the ion–ion recombination rate constant decreases as pressure increases. The rate constant is proportional to the reciprocal of pressure in high-pressure region.

According to the Langevin-Harper formula, the ion–ion recombination rate constant in high-density regions is

$$k_{LH} = 4\pi e\mu \tag{5}$$

where e is the magnitude of the electronic charge and μ is the sum of the mobilities of the positive and negative ions. Mobilities of ions can be calculated using the Boltzmann constant k, the temperature T, and the diffusion coefficient D:

$$\mu = \frac{e}{kT}D \tag{6}$$

The diffusion coefficient in gas phase can be derived from the gas kinetic theory. The coefficient can be expressed using the average velocity $<v>$, the mean free path λ, the temperature T, the density n, and the reduced mass m_u:

$$D = \frac{1}{3}v\lambda = \frac{1}{3}\left(\frac{8kT}{\pi m_u}\right)^{1/2}\left(\frac{1}{\sqrt{2\pi d^2 n}}\right) \tag{7}$$

The numerical factor (1/3) in Equation 7 was obtained from the approximation presented in the gas kinetic theory, and is approximately six times larger than was the experimental measurement [23].

According to the Thomson formula, a recombination occurs when an ion collides with a neutral molecule when an ion of the opposite species is located within a trapping radius r_t. The trapping radius is defined as the magnitude of the potential energy equal to the mean thermal kinetic energy:

$$\frac{e^2}{r_t} = \frac{3kT}{2} \tag{8}$$

The Thomson formula for ion–ion recombination rate constant in low-density regions is

$$k_T = \pi r_t^2 \omega \left(\frac{3kT}{m_u}\right)^{1/2} \tag{9}$$

in which

$$\omega = \omega_1 + \omega_2 \tag{10}$$

$$\omega_i = \frac{4r_t}{3\lambda_i} \tag{11}$$

Subscripts 1 and 2 represent positive ions and negative ions, respectively.

The ion-to-ion recombination rate constants were calculated using the Langevin-Harper formula and the Thomson formula for 2,5-DHB. Ion–ion recombination rate constant as a function of neutral concentration is illustrated in Figure 1.

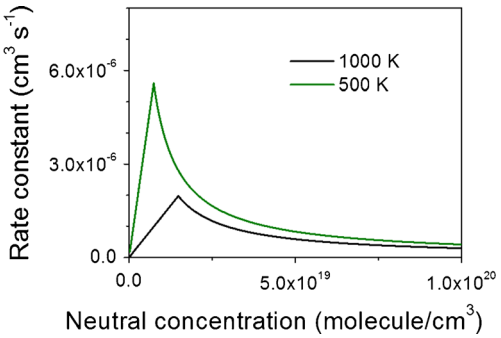

Figure 1. Ion–ion recombination rate constant for 2,5-DHB calculated from the Langevin-Harper formula and the Thomson formula

The loss of ions from ion–ion recombination was calculated using the rate equation

$$\frac{d[ion]}{dt} = k_b[cation][anion] \tag{12}$$

The initial concentrations of the neutrals and ions were the corresponding concentrations in the liquid phase before desorption occurs. As the molecules and ions desorbed from surface, the gas plume expanded in the vacuum rapidly. The change of gas plume volume, and therefore the change of neutral and ion concentrations, as a function of time, was estimated based on the relative velocity and angular distribution from previous experimental measurements [24]. Total ion loss was calculated in 1 ps increments until the gas plume volume was very large, such that ion concentration was too low to undergo recombination. Details of calculation methods using rate equation have been reported in the supplementary material of our previous work [3].

At a low laser fluence where the total desorbed neutral was 2×10^{11} molecules and the ion-to-neutral ratio before desorption was 10^{-8}, the ion loss during gas plume expansion was less than 0.1%. At a high laser fluence where the total desorbed neutral was 1×10^{12} molecules and the ion-to-neutral ratio before desorption was 0.5×10^{-7}, the ion loss during gas plume expansion increased to 1%–5%. The actual values depend on the temperature of gas plume. Only at an extremely high laser fluence where the total desorbed neutral was 8×10^{12} molecules and the ion-to-neutral ratio before desorption was near 10^{-6}, the ion loss during the expansion was as large as 40%. The difference in ion-to-neutral ratios between thermal proton transfer model and the experimental measurements at a high laser fluence, as shown in Figure 2a in [3], may be partially caused by ion–ion recombination. The calculations of ion–ion recombination based on the Langevin-Harper formula and the Thomson formula exhibit orders of magnitude similar to the calculations in our previous study using the gas kinetic hard sphere collision theory, but were substantially smaller than Knochenmuss' calculations.

The ion–ion recombination rate does not depend on how ions are generated, but rather depends on the initial ion concentrations. According to Equation 12, the ion–ion recombination rate is large for large initial ion concentrations; therefore, the fraction

of non-recombined ions is small. In another recent paper, Knochenmuss used molecular dynamics simulation to calculate the ion–ion recombination rate [25]. The ion-to-neutral ratio used in his simulation was 10^{-3}–10^{-4}, which the initial ion concentration was 10^4 times larger than that predicted by thermal proton transfer model. The fraction of non-recombined ions in his molecular dynamics simulation was 2%–7%. According to this molecular dynamics simulation, a much larger fraction of non-recombined ion is expected for low initial ion concentration (e.g., the initial ion concentration from our thermal proton transfer model). The small fraction (6×10^{-6}) of non-recombined ions in Knochenmuss' calculations for a low initial ion concentration using "black sphere" model [10] is contradictory to his early calculations [25] using a molecular dynamics simulation.

Angus Gray-Weale
School of Chemistry
University of Melbourne
VIC 3010, Australia

Chi-Kung Ni
Institute of Atomic and Molecular Sciences
Academia Sinica
Taipei, Taiwan

References

1. Niu, S.F., Zhang, W.Z., Chait, B.T.: Direct comparison of infrared and ultraviolet wavelength matrix-assisted laser desorption/ionization mass spectrometry of proteins. J. Am. Soc. Mass Spectrom. **9**, 1–7 (1998)
2. Chen, X., Carroll, J.A., Beavis, R.C.: Near-ultraviolet-induced matrix-assisted laser desorption/ionization as a function of wavelength. J. Am. Soc. Mass Spectrom. **9**, 885–891 (1998)
3. Chu, K.Y., Lee, S., Tsai, M.T., Lu, I.C., Dyakov, Y.A., Lai, Y.H., Lee, Y.T., Ni, C.K.: Thermal proton transfer reactions in ultraviolet matrix-assisted laser desorption/ionization. J. Am. Soc. Mass Spectrom. **25**, 310–318 (2014)
4. Chu, K.Y., Lee, S., Tsai, M.T., Lu, I.C., Dyakov, Y.A., Lai, Y.H., Lee, Y.T., Ni, C.K.: Erratum to: thermal proton transfer reactions in ultraviolet matrix-assisted laser desorption/ionization. J. Am. Soc. Mass Spectrom. **25**, 1087–1087 (2014)
5. Lu, I.C., Lee, C., Chen, H.Y., Lin, H.Y., Hung, S.W., Dyakov, Y.A., Hsu, K.T., Liao, C.Y., Lee, Y.Y., Tseng, C.M., Lee, Y.T., Ni, C.K.: Ion intensity and thermal proton transfer in ultraviolet matrix-assisted laser desorption/ionization. J. Phys. Chem. B **118**, 4132–4139 (2014)
6. Caillol, J.M., Levesque, D., Weis, J.J.: Electrical properties of polarizable ionic solutions. I. Theoretical aspects. J. Chem. Phys. **91**, 5544–5554 (1989)
7. Caillol, J.M., Levesque, D., Weis, J.J.: Electrical properties of polarizable ionic solutions. II. Computer simulation results. J. Chem. Phys. **91**, 5555–5566 (1989)
8. Lu, I.C., Chu, K.Y., Lin, C.Y., Dyakov Y.A., Hsu, H.C., Lee Y.T., Ni C.K.: Ion-to-neutral ratios and thermal proton transfer reactions in matrix-assisted laser desorption/ionization. Proceedings of the 62nd ASMS Conference on Mass Spectrometry and Allied Topics, June 15–19. American Society of Mass Spectrometry, Baltimore, Maryland. p. 1074 (2014)
9. Lu, I.C., Chu, K.Y., Lin, C.Y., Shang-Yun, Wu, Dyakov Y.A., Chen, J.J., Gray-Weale, A., Lee Y.T., Ni C.K.: Ion-to-neutral ratios and thermal proton transfer in matrix-assisted laser desorption/ionization. J. Am. Soc. Mass. Spectrom. **26**, 1242–1251 (2015)
10. Knochenmuss, R.: Energetics and kinetics of thermal ionization models of MALDI. J. Am. Soc. Mass Spectrom. **25**, 1521–1527 (2014)
11. Marcus, Y.: The structuredness of solvents. J. Solut. Chem. **21**, 1217–1230 (1992)
12. Atkins, P., de Paula, J.: Atkins' Physical Chemistry, 8th edn, pp. 624–627. Oxford University Press, Oxford (2006)
13. Bromberg, J.P.: Physical Chemistry, 2nd ed. W. H. Freeman and Company, New York, p. 850 (1984)
14. Pollock, E.L., Alder, B.J., Patey, G.N.: Static dielectric properties of polarizable Stockmayer fluids. Phys. A: Stat Mech Appl. **108**, 14–26 (1981)
15. Madden, P., Kivelson, D.: A Consistent molecular treatment of dielectric phenomena. Adv. Chem. Phys. **56**, 467–566 (1984)
16. Gray-Weale, A.: Calculations of the relative permittivity for modelling MALDI. (in preparation)
17. Dashtiev, M., Wafler, E., Rohling, U., Gorshkov, M., Hillenkamp, F., Zenobi, R.: Positive and negative analyte ion yield in matrix-assisted laser desorption/ionization. Int. J. Mass Spectrom. **268**, 122–130 (2007)
18. Hillenkamp, F., Wafler, E., Jecklin, M.C., Zenobi, R.: Positive and negative analyte ion yield in matrix-assisted laser desorption/ionization revisited. J. Mass Spectrom. **285**, 114–119 (2009)
19. Kotomin, E., Kuzovkov, V.: Phenomenological kinetics of Frenkel defect recombination and accumulation in ionic solids. Rep. Prog. Phys. **55**, 2079–2188 (1992)
20. Bated, D.R., Flannerys, M.R.: Three-body ionic recombination at moderate and high gas densities. J. Phys. B: Atom. Mol. Phys. **2**, 184–190 (1969)
21. Bated, D.R.: Ionic recombination in a high density ambient gas. J. Phys. B: Atom. Mol. Phys. **8**, 2722–2727 (1975)
22. Mezyk, S.P., Cooper, R., Sherwellt, J.: Ion recombination rates in rare gas cation-halide anion systems. 3. XeBr and XeI. J. Phys. Chem. **97**, 9413–9419 (1993)
23. Houston, P.L.: Chemical Kinetics and Reaction Dynamics, 1st edn, pp. 131–132. McGraw-Hill, New York (2001)
24. Tsai, M.T., Lee, S., Lu, I.C., Chu, K.Y., Liang, C.W., Lee, C.H., Lee, Y.T., Ni, C.K.: Ion-to-neutral ratio of 2,5-dihydroxybenzoic acid in matrix-assisted laser desorption/ionization. Rapid Commun. Mass Spectrom. **27**, 955–963 (2013)
25. Knochenmuss, R., Zhigilei, L.V.: What determines MALDI ion yields? A molecular dynamics study of ion loss mechanisms. Anal. Bioanal. Chem. **402**, 2511–2519 (2012)